Forecasting Ocean Waves off the U.S. East Coast Using an Ensemble Learning Approach

Nazanin Chaichitehrani*, Ruoying He, Mohammad Nabi Allahdadi

Department of Marine, Earth, and Atmospheric Sciences, North Carolina State University
Raleigh, North Carolina, USA

*Corresponding author: nchaichi@gmail.com

Abstract

This study introduces an ensemble learning model for the prediction of significant wave height and average wave period in stations along the U.S. Atlantic coast. The model utilizes the stacking method, combining three base learner models - Lasso regression, support vector machine, and Multi-layer Perceptron - to achieve more precise and robust predictions. To train and evaluate the models, a twenty-year dataset comprising meteorological and wave data was used, enabling forecasts for significant wave height and average wave period at 1, 3, 6, and 12 hour intervals. The data collection involved two NOAA buoy stations situated on the U.S. Atlantic coast. The findings demonstrate that the ensemble learning model constructed through the stacking method yields significantly higher accuracy in predicting significant wave height within the specified time intervals.

Moreover, the study investigates the influence of swell waves on forecasting significant wave height and average wave period. Notably, the inclusion of swell waves improves the accuracy of the 12-hour forecast. Consequently, the developed ensemble model effectively estimates both significant wave height and average wave period. The ensemble model outperforms the individual models in forecasting significant wave height and average wave period. This ensemble learning model serves as a viable alternative to conventional coastal models for predicting wave parameters.

Early Online Release: This preliminary version has been accepted for publication in *Artificial Intelligence for the Earth Systems*, may be fully cited, and has been assigned DOI 10.1175/AIES-D-23-0061.1. The final typeset copyedited article will replace the EOR at the above DOI when it is published.

1. Introduction

Accurate prediction of wave characteristics plays a crucial role in various applications such as wave energy development, marine facility security, fishery management, offshore and coastal structure design, and coastal protection (Jain et al., 2011; Moghaddam et al., 2018; Gracia et al., 2021; Isaee Moghaddam et al., 2021; Ahn et al., 2022). While conventional numerical wave models like Simulating WAves Nearshore (SWAN; Booij et al. 1999) have been widely used for forecasting ocean wave parameters (e.g., Allahdadi et al., 2017; Li et al., 2020; Chaichitehrani et al., 2022; Sapiega et al., 2023), they are limited by high computational requirements and small time step constraints when dealing with complex oceanic processes. Moreover, the predictions of these models may lack generalization across different oceans and seas (Kumar et al., 2018).

To address these challenges, machine learning approaches have gained significant attention in recent decades, leveraging the abundance of available data for predicting wave characteristics. These data-driven and model-free methods offer an alternative or complementary approach to conventional numerical wave models (Elbisy, 2015; Mooneyham et al., 2020; Ghadami and Epureanu, 2022; Zhan et al., 2022). Machine learning (ML) methods have shown success in predicting wave characteristics, particularly in emergency situations where prompt results are crucial (Fan et al., 2020). Various sources of data, including numerical wave models, buoys, and weather stations, have been extensively utilized in ML models for wave parameter prediction. Neural network techniques, known for their computational efficiency, have been widely employed in wave forecasting studies (Tolman et al., 2005; Londhe and Panchang, 2006; Pooja et al., 2011; Kumar et al., 2018). Other data-driven models, such as artificial neural networks (ANN) and convolutional neural networks (CNN), have been particularly popular for wave parameter forecasting, enabling predictions without prior system knowledge. For instance, Sadeghifar et al. (2017) demonstrated the robust predictive ability of recurrent neural networks (RNN) in forecasting significant wave height in the southern Caspian Sea using observational data. Long Short-Term Memory (LSTM) models have also been widely employed for wave forecasting in various bodies of water worldwide (Pirhooshyaran and Snyder, 2020; Ahn et al., 2022). Ahn et al. (2022) explored the effectiveness of a multi-task LSTM architecture for global forecasting of significant wave height, achieving promising results in a complex system. While LSTM models are designed to handle long-term dependencies, they may face challenges related to parallelization and training time, thus requiring substantial memory resources. In contrast, simpler ML models like Support

Accepted for publication in *Artificial Intelligence for the Earth Systems*. DOI 10.1175/AIES-D-23-0061.1.

Vector Regression (SVR), Support Vector Machines (SVMs), and Extreme Gradient Boosting (XGB) have been extensively used for wave parameter forecasting due to their simplicity and reduced number of parameters (Mahjoobi and Adeli Mosabbeb, 2009; James et al., 2018; Hu et al., 2021). Berbić et al. (2017) compared the performance of ANN and SVM in predicting significant wave height and found them to be comparable, with ANN exhibiting slightly better accuracy. Garcia et al. (2021) employed Multi-Layer Perceptron (MLP), LightGBM, and ensemble models to enhance the accuracy of numerical models in wave parameter forecasting, achieving a significant reduction in prediction error. Recent studies have also focused on specific regions, such as the Atlantic coast. Wei (2021) applied LSTM models to predict wave parameters at four NDBC stations along the U.S. Atlantic coast. They found that short-term forecasts (e.g., 1 to 6 hours) exhibited higher accuracy than longer-term forecasts (e.g., 24 to 48 hours).

Each of the ML approaches mentioned above has its own strengths and weaknesses. However, relying on a single ML model to predict wave parameters can lead to suboptimal results due to uncertainties in training parameters. To address this issue, ensemble machine learning (EML) models have been developed to mitigate modeling errors and reduce overfitting problems (Berkhahn et al., 2019; Zounemat-Kermani et al., 2020; Tan, 2021). These ensemble models combine predictions from multiple ML models or base/weak learners to improve overall performance and reliability in wave parameter predictions. EML models can overcome individual models' limitations, including statistical, computational, and representation problems (Dietterich, 2000; Zounemat-Kermani et al., 2021). For instance, Kumar et al. (2018) proposed an ensemble extreme learning method for predicting daily wave height, demonstrating the advantages of EML over base learners. By leveraging the collective knowledge of multiple base learners, EML models offer improved predictive performance and enhanced robustness in wave parameter forecasting tasks.

Despite the effectiveness of EML models, there is a lack of comprehensive studies highlighting the potential of EML approaches in predicting wave parameters. This study aims to evaluate the performance of a stacking ensemble approach utilizing three base learners: Lasso Regression, Multi-Layer Perceptron (MLP), and Support Vector Machine (SVM) for the forecasting of short-term (1, 3, 6, and 12 hour) wave characteristics, including significant wave height and average wave period, along the U.S. East Coast. The primary objective is to demonstrate the effectiveness and predictive capabilities of the ensemble learning model in capturing the

Accepted for publication in *Artificial Intelligence for the Earth Systems*. DOI 10.1175/AIES-D-23-0061.1.

temporal variations of wave parameters in a coastal region. The goals of this study are 1) assessing the effectiveness of the three base learners in wave parameter forecasting, and 2) developing and evaluating the performance of the stacking ensemble learning model. In addition to investigating various ML techniques, this study introduces an innovative approach to enhance the accuracy of wave parameter forecasts: the incorporation of swells height components at each station as an additional training parameter. This improves the predictive capabilities of the models. By integrating this novel methodology into the analysis, the study aims to enhance the forecast accuracy of wave parameters.

2. Study Region and Data

Our study focused on forecasting significant wave height and average wave period using data from two locations along the U.S. East Coast: the Cape Hatteras region and a portion of the South Atlantic Bight (Figure 1). The wave climate in this region exhibits a seasonal pattern, with easterly to southeasterly seas (wind-generated waves) and swells during summers, and a northerly to northeasterly wind field produced by strong storms, known as nor'easters, during the winter and early spring (Allahdadi et al., 2019a and b). Allahdadi et al. (2019b) emphasized the significant spatial variability of the wind field in this region due to its large geographical extent. Consequently, different regions of the wave growth curve, such as fetch-limited, fully developed, and duration-limited, can be observed at various locations depending on their proximity to a storm center, as described by Kahna and Clayton (1994) and the Coast Engineering Manual (2000). The occurrence of tropical storms during the summer and early fall in the western Atlantic further adds complexity to the wave fields. Thus, utilizing datasets with appropriate quality and temporal coverage is crucial for accurate model training and forecasts.

To obtain the necessary data, we collected meteorological, wave parameter, and wave spectral data from April 1, 2003, to December 1, 2022, from two stations operated by the NOAA National Data Buoy Center (NDBC) (https://www.ndbc.noaa.gov/). The dataset includes various measurements such as wind direction (degrees), wind speed (m/s), wind gust (m/s), significant wave height (m), dominant wave period (seconds), average wave period (seconds), direction of the dominant wave periods (degrees), sea level pressure (hPa), air temperature (degrees Celsius), sea surface temperature (degrees Celsius), and dew point temperature (degrees Celsius). These data were used through a selection process to find the input variables (features or predictors) to forecast significant wave height and average wave period at stations 41025 and 41013 on the U.S. Atlantic

Accepted for publication in *Artificial Intelligence for the Earth Systems*. DOI 10.1175/AIES-D-23-0061.1.

coast (Figure 1 and Table 1). The length of the data required for training can vary significantly based on several factors, including the nature of the data, the complexity of the model, and the project goal (Gütter et al., 2022; Dawson et al., 2023). Accordingly, the minimum required length of data should be determined. For an ML-based wave model, the goal may necessitate considering seasonal and multidecadal variations, as well as the frequency of extreme events, when selecting the minimum length of data. If the available data is insufficient, it is advisable to confirm whether the dataset is indeed too small and consider collecting more data. Additionally, exploring data augmentation methods could artificially increase your sample size.

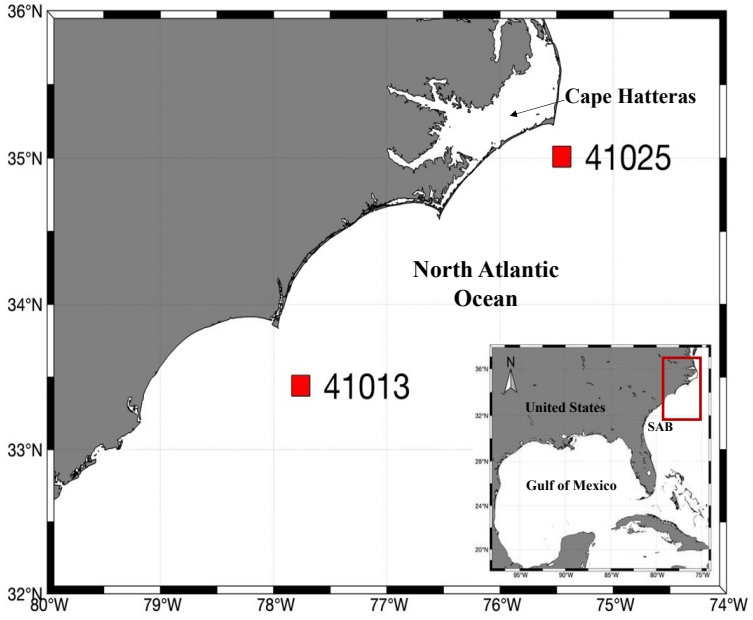

FIG. 1. Location of NOAA NDBC stations 41025 and 41013. SAB stands for South Atlantic Bight.

TABLE 1. The NOAA NDBC stations' information used to forecast significant wave height and wave periods.

Station Id	Station name	Longitude	Latitude	Water Depth (m)
41025	Diamond Shoals, NC	-75.45	35.01	48.8
41013	Frying Pan Shoals, NC	-77.76	33.441	33

Twelve variables were initially examined as potential predictors to forecast significant wave heights and average wave periods for the next 1, 3, 6, and 12 hours (Table 2). Additionally, this study employed an approach to account for the influence of swells on the forecast of wave height and period.

Accepted for publication in *Artificial Intelligence for the Earth Systems*. DOI 10.1175/AIES-D-23-0061.1.

Through wave spectrum analysis, we determined that the wave field in our study area is influenced not only by local wind but also by swells originating from distant locations. As a result, including these swells in our analysis became essential in capturing the complete wave climate of our study area for forecast times 12 hours and larger.

TABLE 2. Twelve variables used, including input variables (predictors) used to forecast targets. The targets are significant wave height (WVHT or Hs) and average wave period. Except for swells and seas, the data were obtained from NOAA National Buoy Data Center (http: //www.ndbc.noaa.gov/measdes.shtml).

Variable	Description	Unit	Predictor (P) or Target (T)
APD	Average wave period	seconds	T
ATMP	Air temperature	degrees Celsius	P
DEWP	Dewpoint temperature	degrees Celsius	P
DPD	Dominant wave period	seconds	P
GST	Gust speed	m/s	P
PRES	Sea level pressure	hPa	P
Seas Height	Heights of waves generated by local wind	meters	P
Swell Height	Heights of waves generated by distance wind	meters	P
WDI	Wind direction	degrees	P
WSP	Wind speed	m/s	P
WTMP	Water temperature	degrees Celsius	P
WVHT	Significant wave height	meters	T

Wave and wind vectors in the study area do not have a distinct pattern due to the varied forces influencing them (Figure 2). Station 41025 exhibits two dominant wind directions, one from the north-northeast and the other from the southwest, aligning with the general coastline orientation near this station. The north-northeast winds account for approximately 20% of the wind occurrences, while the southwest winds constitute around 17%. Conversely, at station 41013, winds predominantly blow from the northeast and southwest directions, with occurrence of 22% and 20%, respectively. The temporal variability in wind speed and direction at each station presents a challenge for the machine learning model in capturing these diverse wind patterns accurately. The wave directions (Figures 2C and D) do not consistently align with the wind directions. This disparity between wind and wave directions further highlights the complexity of the wave dynamics in the study area. At station 41025, the predominant wave directions fall within the northeast to east

Accepted for publication in *Artificial Intelligence for the Earth Systems.* DOI 10.1175/AIES-D-23-0061.1.

range, whereas at station 41013, they lie within the east to southeast range. This pattern can be attributed to various factors such as the geometry of the coastline (Ardhuin et al., 2007), variations in fetch lengths in different directions (Massel, 1990), and the influence of remotely generated waves (swells) (Ahn et al., 2021) at each location. These findings emphasize that achieving a highly accurate machine learning forecast model may require the inclusion of additional parameters and considerations beyond wind speed and direction alone.

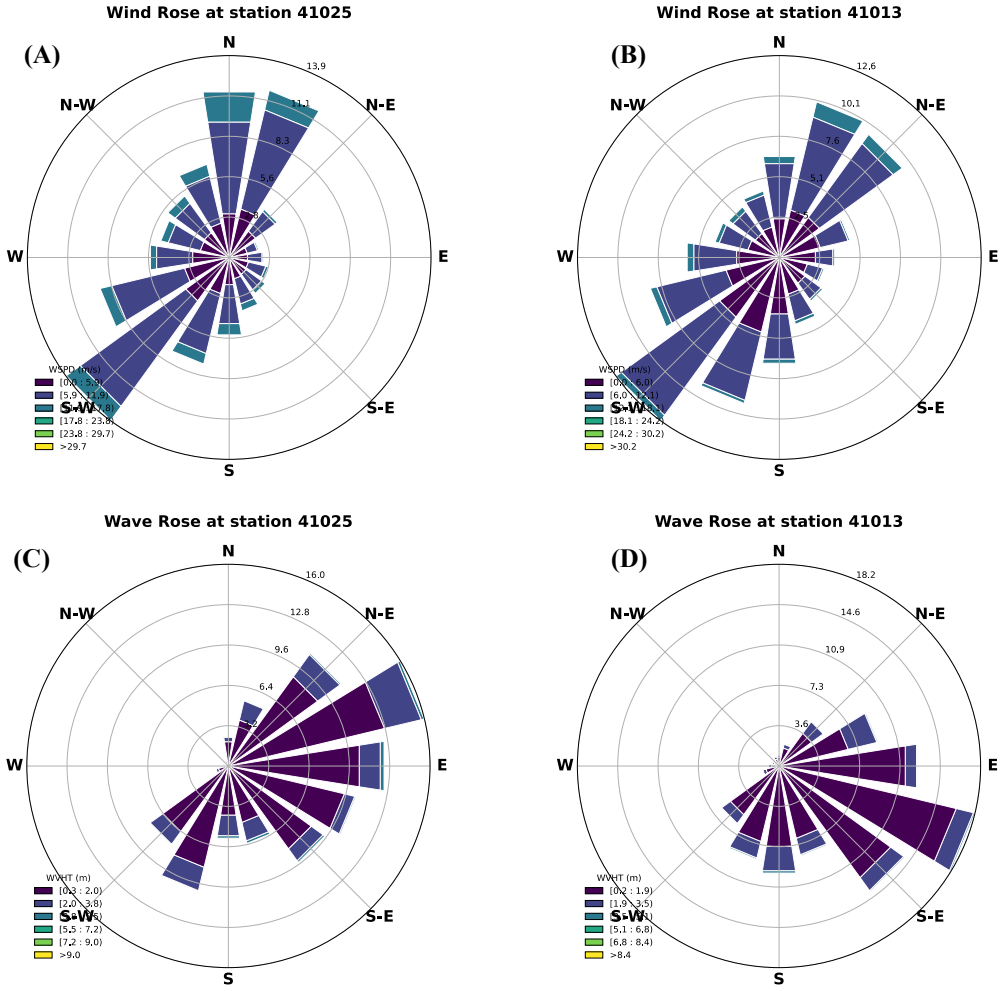

FIG. 2. Wind (A and B) and wave (C and D) rose plots at stations 41025 (A and C) and 41013 (B and D) from April 1, 2003, to December 1, 2022.

The energy distribution within the frequency-directional space provides insights into the various wave components originating from different directions that contribute to the overall wave parameters. Portions of the wave energy do not align with the prevailing local wind direction and

Accepted for publication in *Artificial Intelligence for the Earth Systems*. DOI 10.1175/AIES-D-23-0061.1.

are likely generated by distant winds (swells). 2D spectra of wave energy distribution at the two stations visually highlight the presence of wave components originating from different directions and highlight the complexity of the wave field (Figure 3).

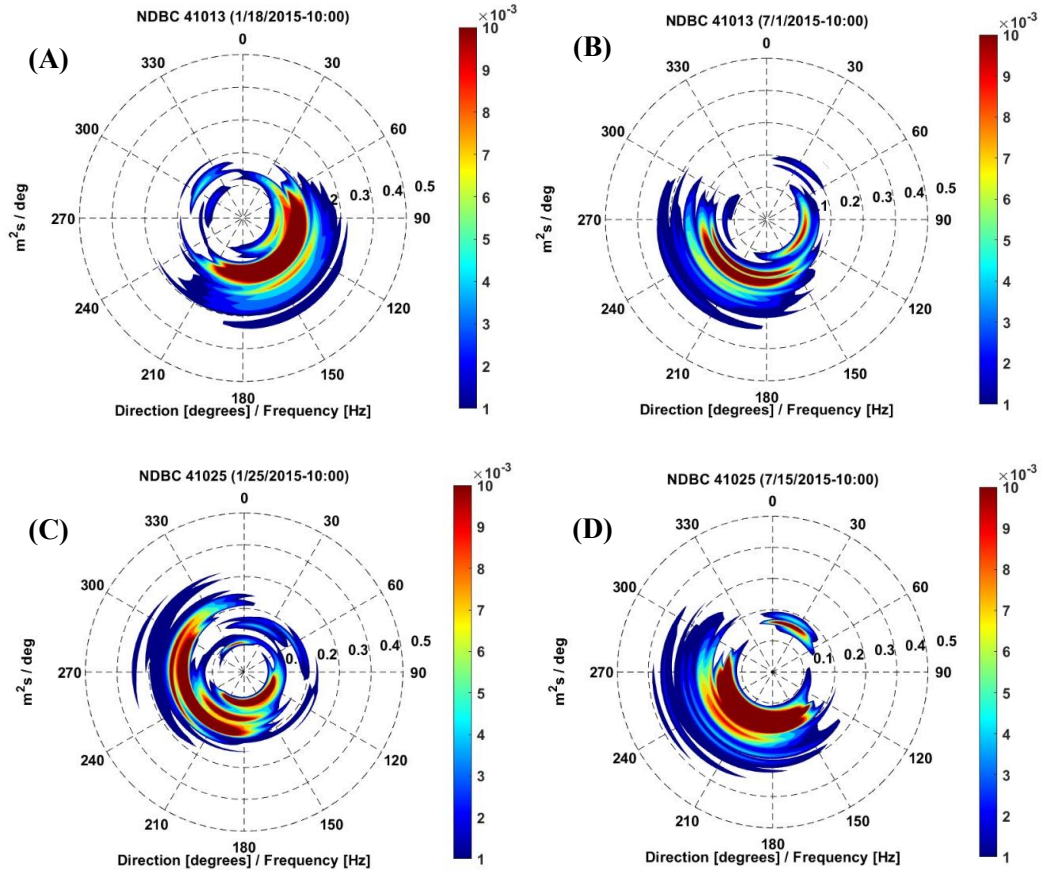

FIG. 3. Examples of frequency-direction spectra measured at stations 41013 (A and B) and 41025 (C and D) on specific days.

The observed spectra at both stations and different time periods clearly indicate the presence of significant energy sectors beyond the main energy sectors aligned with the local wind direction. These additional energy sectors, spanning various directions and frequency bands, represent waves that are not locally generated and can be identified as swells. For example, at station 41025, a complex wave energy spectrum was observed on 01/25/2015 at 10:00 UTC (Figure 3C). While a considerable portion of the wave energy aligned with the southwest to west direction, which corresponds to the local wind direction, several other high-energy sectors were evident. Notably, a distinct low-frequency wave energy sector with a southeast direction indicated the presence of a

Accepted for publication in *Artificial Intelligence for the Earth Systems*. DOI 10.1175/AIES-D-23-0061.1.

primary swell component. Additionally, other swell components originating from the north and south were identified, all characterized by lower frequencies than the primary wind-generated energy.

Further analysis of the 2D spectra at these stations for various months and days revealed numerous instances of spectra with multiple peaks in different directions. It became apparent that accurately describing these spectra solely based on the local wind within a machine learning framework was challenging. Consequently, this observation motivated us to separate the swell component and incorporate it as an additional predictor, which will be elaborated upon in the following sections.

3. Methods

a. Feature Selection

In the context of wave parameter forecasting using machine learning techniques, an initial step is to determine the impact of each available parameter (feature variable) on estimating wave parameters. Feature selection plays a crucial role in machine learning, as optimal feature selection enhances model accuracy, reduces computational costs, and facilitates the understanding and interpretation the relationship between feature variables and target variables. In this study, feature selection was carried out using a correlation matrix method, which assesses the relevance of each feature variable by examining its association with the target variables and other feature variables. This allows the identification of informative features that significantly contribute to the forecast of wave parameters. Along with the standard NDBC parameters, additional feature variables such as swells and sea height were included. Swells and seas parameters were calculated using the approach described in Section b. These supplementary variables were incorporated to enhance the model's predictive capabilities and capture a more comprehensive understanding of the wave system.

Correlation analysis was performed with feature variables and the target variables significant wave height (WVHT) and average wave period (APD). The dependencies between each feature and target variable were visualized using Pearson correlation heat maps (Figure 4). The correlation analysis was conducted for various forecast times for 1, 3, 6, and 12 hours. The target variables (WVHT and APD) correspond to the same feature variables, but their values are time-shifted according to the chosen forecast time (1, 3, 6, 12 h).

Figure 4 illustrates the correlation matrix between the feature and target variables, with a focus on the 1-hour and 12-hour forecasts at station 41025. Similar correlation patterns were

Accepted for publication in *Artificial Intelligence for the Earth Systems*. DOI 10.1175/AIES-D-23-0061.1.

observed for the 1-hour and 12-hour forecasts at station 41013. The Pearson correlation coefficient ranges from 1, indicating a strong positive correlation, to 0, indicating a weak or no correlation. Importantly, our study included swells and seas wave height as feature variables, specifically limited to the forecast of wave parameters for the next 12 hours. This decision was based on an understanding of the dynamics of swells formation and propagation, which suggests that their impacts become more pronounced over longer forecast periods.

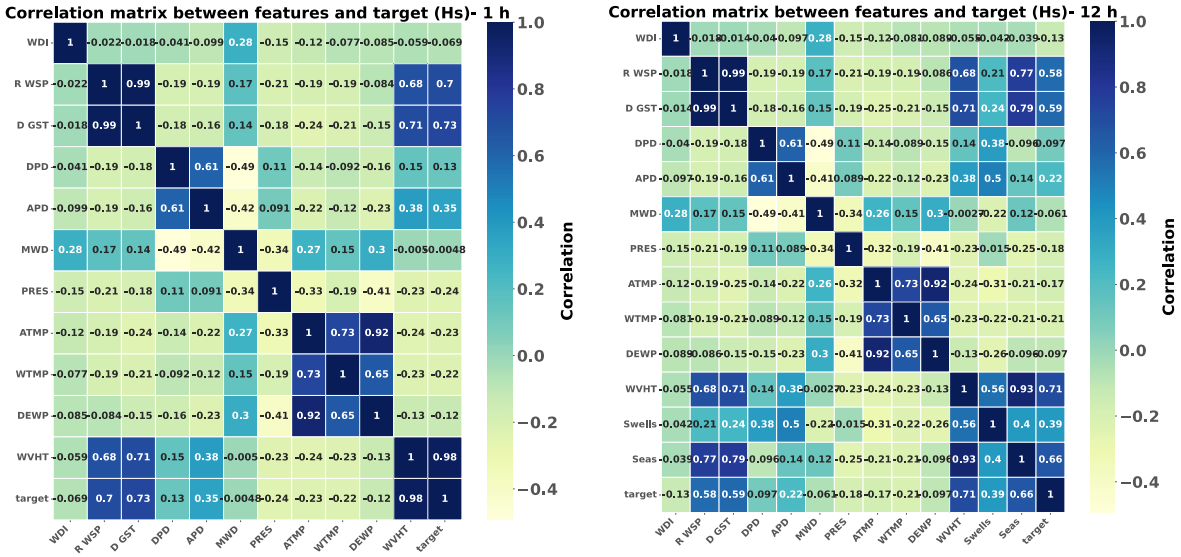

FIG. 4. Pearson correlation heat maps between features and target (significant wave height) for the 1 h (left) and 12 h (right) forecast at station 41025.

The analysis revealed that wave height, wind speed, gust speed, and mean wave period are the most influential parameters contributing to the forecast of the target variables at both stations. Therefore, these four parameters were employed for the final model training and forecasting. Additionally, for the 12 hour forecast, swells wave height was included. These parameters displayed positive correlations with the wave parameters, indicating their significance in predicting wave characteristics. Conversely, other meteorological and oceanographic parameters, such as air pressure, air temperature, and water temperature, demonstrated either negative correlations or very weak correlations with the wave parameters. It is important to note that the negative difference between air temperature and water temperature could potentially contribute to increased wind energy transfer to the water surface, resulting in higher wind-generated wave height, as reported by Ardhuin et al. (2007) and Allahdadi et al. (2019). However, investigating this effect within the machine learning framework falls outside the scope of this study.

Accepted for publication in *Artificial Intelligence for the Earth Systems*. DOI 10.1175/AIES-D-23-0061.1.

Furthermore, the calculated seas and swells components exhibited relatively high correlations, with values reaching as high as 0.6 - 0.7 in forecasting wave height. This highlights the significance of considering these components as predictors in the wave parameter forecasts. Frequency histograms of the feature parameters at station 41025 exhibit diverse distributions (Figure 5). Parameters such as wave height, wind speed, and wave periods, which display high correlations with the target parameters, generally exhibit left-skewed distributions. On the other hand, parameters such as air pressure or air temperature, which exhibit lower correlations with the target parameters, generally show right-skewed or nearly normal distributions. This consistency between the histograms of the feature and target parameters could serve as a preliminary indicator for selecting the final feature parameters in a machine learning practice.

Regarding the wind data, it should be noted that wind direction has a cyclic nature and, therefore, that correlation with wave height can be higher if wind components are used along with wave components when establishing Pearson correlation. In our model training and forecasts of wave parameters, we tried both options (wind speed and direction vs. wind velocity components) and found no meaningful difference. The results presented in the next section are based on the model using wind components.

It should be noted the high correlation between certain parameters, such as wave period and wave height, or vice versa, does not necessarily imply that they are predictors of each other. Instead, it indicates their association and the fact that similar forcing mechanisms primarily influence them. However, in this study, the wave period was utilized in model training as a predictor for wave height, and vice versa. This is due to the fact that wave period is a highly non-linear function of the wave spectral moments (0^{th}, -1^{th}, or -2^{th}, depending on the definition). Along with wave height, which is a function of the 0^{th} spectral moment, these parameters can convey aspects of the non-linear and spectral nature of waves to the trained model. This is particularly useful when dealing with highly non-uniform wind fields over the study region. Notably, similar approaches have been employed in several other research studies, including those by Wei et al. (2021), Shi et al. (2023), and Zhan et al. (2022).

Accepted for publication in *Artificial Intelligence for the Earth Systems.* DOI 10.1175/AIES-D-23-0061.1.

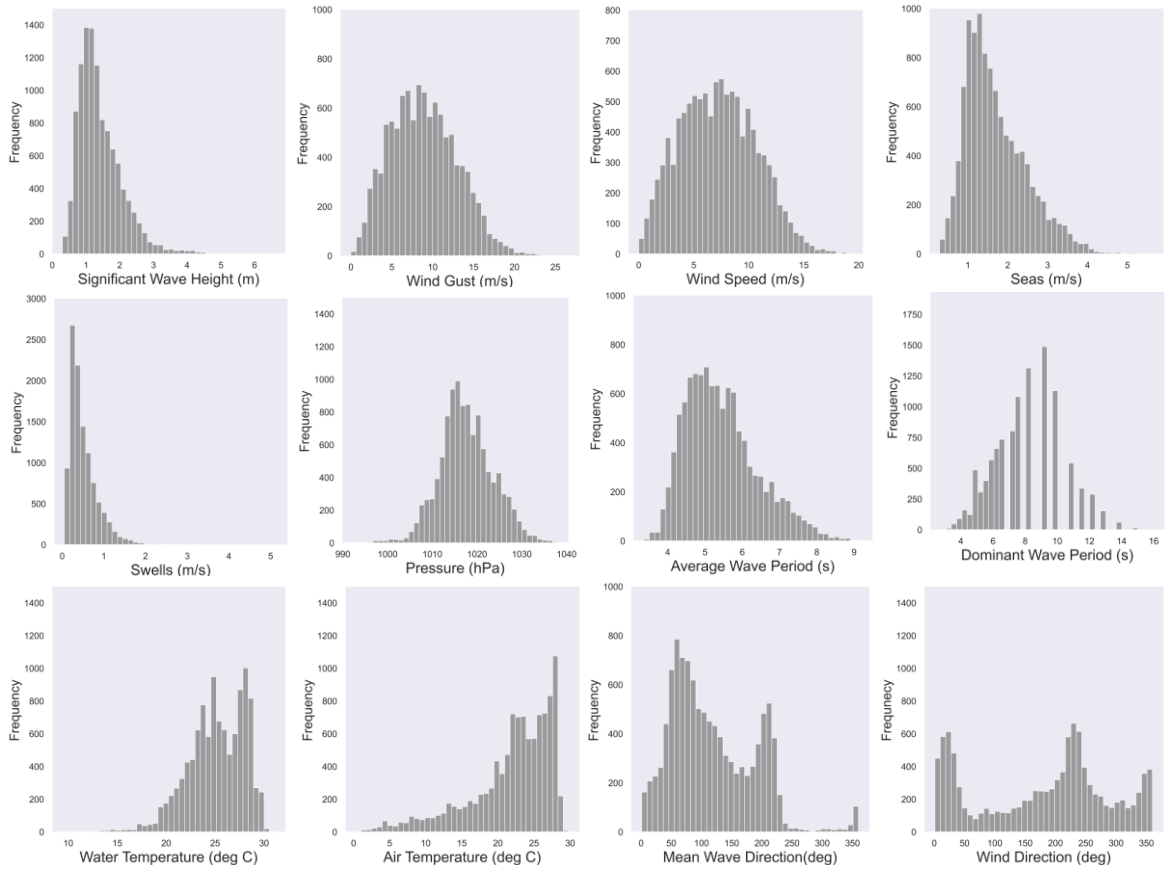

FIG. 5. Distribution of features at station 41025.

Regarding the approach used in this study for feature and predictor selection, the results can likely be used only for short-term wave forecasts up to 24-48 hours. Hence, in addition to wind parameters, wave parameters of the present time are also used as predictors of future wave events. One of the main reasons for adopting this approach is the inherently non-linear process of wave generation by wind, which does not guarantee a strong correlation between wave parameters and wind speed (Allahdadi et al., 2019a). In fact, the non-uniformity of wind fields over the U.S. East Coast and offshore regions, coupled with the complex coastal geometry, significantly contributes to the observed low correlation between wind speed and wave parameters.

Accepted for publication in *Artificial Intelligence for the Earth Systems.* DOI 10.1175/AIES-D-23-0061.1.

b. Separation of Seas and Swell Waves

Wind is the primary force responsible for generating gravity waves; consequently, wind should be used as the main feature parameter for model training and forecasting. However, once generated by wind, waves can travel hundreds to thousands of kilometers as swells, even in the absence of direct wind force (Ardhuin et al., 2009). These swells travel at a group speed while their energy is basically conserved (Ardhuin et al., 2009). This implied that in regions characterized by a predominant swell wave climate, the wave parameters are not necessarily consistent with wind parameters (Gulev and Grigorieva, 2009). Depending on the season and/or geographical location, swells can be an important or even dominant component of the wave energy spectrum. For example, in the northern Indian Ocean, including the Arabian Sea and the Gulf of Oman, swells dominate the wave characteristics during the summer monsoon season (Chaichitehrani and Allahdadi, 2018). In the tropical and mid-latitude offshore regions of the North Atlantic, an analysis of satellite and modeling data from 2002 to 2008 revealed the predominant influence of swells throughout the year (de Farias et al., 2012). In many previous studies covering extensive oceanic basins, especially within the study region along the U.S. East Coast, regardless of the importance of remotely generated waves (swells), swells have not been used in model training and the prediction of wave parameters. However, in addition to wind as the primary wave-generating force, the inclusion of swells may be essential.

Although this assumption may be valid for small, enclosed basins, it is not applicable to the vast geographical extent of the U.S. East Coast. As depicted in Figure 3, significant portions of the energy spectrum exhibit deviations from the general wind direction. These deviations correspond to swells, which are waves originating from remote locations and propagating towards the study area. In the case of implementing the forecasts for an area with gridded data and well-defined open boundaries, one approach to taking the swell effect into account is to include wave data along the open boundaries, obtained as the output from a numerical model, into model training and use it as a predictor. This approach was successfully applied in Monterey Bay by James et al. (2017). However, as we are applying the ML framework to only two observational points without a specific offshore boundary in our study, this approach is not applicable. Instead, we adopted the methods developed by Wang and Hwang (2001) and Hwang et al. (2012) to separate wind-generated seas from the swell wave components. We effectively incorporated the swell component into our

Accepted for publication in *Artificial Intelligence for the Earth Systems.* DOI 10.1175/AIES-D-23-0061.1.

analysis by utilizing spectral data measured at the study stations. This swell component and other predictors (Table 2) were treated as independent parameters during the model training process. By including the swell component, we aimed to enhance the accuracy and robustness of our ML model in capturing the diverse wave dynamics experienced along the U.S. East Coast.

The seas and swell waves components were separated following Wang and Hwang (2001):

$$H_{sw} = 4\sqrt{m_{0w}} \quad (1)$$

$$m_{nw} = \int_{f_s}^{f_{max}} f^n S(f) df, \;\; n = 0, 2 \quad (2)$$

$$H_{ss} = 4\sqrt{m_{0s}} \quad (3)$$

$$m_{ns} = \int_{f_{min}}^{f_s} f^n S(f) df, \;\; n = 0, 2 \quad (4)$$

where H_{sw} and H_{ss} are significant wave height of the sea and swell components, respectively. f_s is the separation frequency, and f_{max} and f_{min} are the maximum and minimum measured frequencies. f_s is defined as (Hwang et al., 2012):

$$f_{s1} = 24.2084 f_{m1}^3 - 9.2021 f_{m1}^2 + 1.8906 f_{m1} - 0.04286 \quad (5)$$

where f_{m1} is the peak frequency of $I_1(f)$

$$I_1(f) = \frac{m_1(f)}{\sqrt{(m_{-1}(f))}} \quad (6)$$

Where $m_1(f)$ is the first moment of the wave spectrum:

$$m_n(f) = \int_f^{f_u} f'^n S(f') df' \quad (7)$$

where $n = 1$, and the upper frequency for separation seas and swells is $f_u = 0.5\ Hz$.

The calculated swells and seas wave heights at each station were included as predictors to forecast significant wave height and average wave period. Timeseries of total significant wave height compared to the swell wave heights (Figure 6) reveal that, depending on the season, swell height can account for a significant portion of total wave height up to one-third to half of it. This underscores the importance of considering the swell component in wave height predictions, as it can substantially impact the overall wave climate and wave parameter forecasts along the U.S. East Coast. We conducted two sets of forecasts: one considering the swell component of the wave spectrum during model training and another excluding it. The purpose was to evaluate the extent to which including the swell information improves the accuracy of the forecasts. The swell

Accepted for publication in *Artificial Intelligence for the Earth Systems*. DOI 10.1175/AIES-D-23-0061.1.

components were solely incorporated for the 12 hour forecasts of significant wave height at both stations.

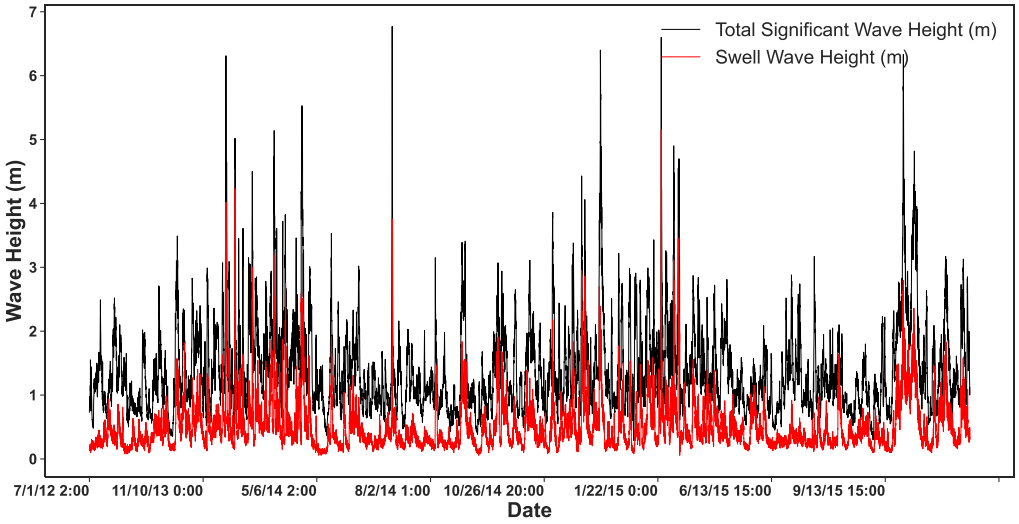

. 6. An example of timeseries of total significant wave height (black line) and swell wave height (red line) over the study period (2012 – 2015).

We investigated the impact of swells on wave parameter forecasts across all forecast horizons, including 1, 3, 6, and 12 hours. However, for forecast horizons shorter than 12 hours, the specific geographical locations of the two stations within the regional wave field in the northwest Atlantic, combined with the rapid propagation of swell waves, render their influence negligible. Consequently, for 1, 3, and 6-hour forecasts, we have presented results exclusively for scenarios involving wind-generated waves, with the effect of swells excluded.

c. Machine Learning Models

A crucial aspect of ML modeling is selecting suitable ML models that effectively capture the variations of target parameters within a specific geographical region. ML models can differ in their architectural design and data processing techniques, resulting in varying performance. Base learner models such as support vector regression (SVR), support vector machines (SVMs), and XGBoost have been widely utilized for wave parameter forecasting due to their simplicity and demonstrated effectiveness (Mahjoobi and Adeli Mosabbeb, 2009; James et al., 2018; Hu et al., 2021). This study employed three base learner models: 1. Least Absolute Shrinkage and Selection Operation (Lasso) regression, 2. Support Vector Machine (SVM), and 3. Multi-Layer Perceptron (MLP). These models were selected based on their proven effectiveness in wave parameter forecasting and their ability to capture variations within our geographical region of interest. The

Accepted for publication in *Artificial Intelligence for the Earth Systems*. DOI 10.1175/AIES-D-23-0061.1.

utilization of these models allows us to leverage their strengths and enhance the accuracy of our predictions in capturing the complex dynamics of wave parameters. Lasso Regression (L1 regularization technique) is a simple model that employs a shrinkage technique, resulting in a smaller set of parameters and facilitating model interpretation. Support Vector Machine (SVM) is designed to separate different classes of data points by identifying an optimal line (hyperplane) that is positioned at an optimal distance from the classes. SVM relies on kernel functions, and in our study, the radial basis function (rbf) kernel yielded the best performance among the available options. SVM with the rbf kernel can capture complex non-linear relationships in the data. In addition, SVMs are effective in high-dimensional spaces and are robust to outliers since they focus on support vectors. SVM naturally incorporates regularization, which can prevent overfitting. In a stacked ensemble, SVMs with rbf kernels can serve as powerful base models for capturing non-linear patterns in the data (Salcedo-Sanz et al., 2014; Martins et al., 2016). Multi-Layer Perceptron (MLP) is a supervised learning algorithm that excels at solving non-linear problems. Its architecture consists of input, hidden, and output layers, with the hidden layers acting as the computational engine. The backpropagation technique is employed to train all the MLP nodes. MLPs can learn complex and hierarchical features from data. They excel in tasks with intricate patterns and large amounts of data. MLPs are particularly useful when the underlying data has intricated, non-linear relationships that other base models might struggle to capture. In a stacked ensemble, an MLP can be one of the base models to provide diversity and complementarity to the ensemble. MLPs excel at representation learning and handling large-scale, complex datasets, making them suitable when the data exhibits high-dimensional and non-linear characteristics (Kim and Adali, 2002; Alsmadi et al., 2009; Kruse et al., 2022). By combining these models with others in a stacked ensemble, we can leverage the strengths of each base model to improve overall predictive performance and handle a wider range of data patterns effectively. These three methods have distinct architectures, learning algorithms, and advantages in forecasting techniques that, when combined, enhance the accuracy and robustness of the forecasts.

An ensemble model was developed using the stacking or stacked generalization method to achieve this. The stacking method utilizes a meta-learner, which learns how to effectively combine the predictions from the base models. The meta-learner acts as the coordinator, using the predictions from the base models as input data and combining them effectively to produce the final prediction.

Accepted for publication in *Artificial Intelligence for the Earth Systems.* DOI 10.1175/AIES-D-23-0061.1.

The dataset was divided into two portions: a training dataset comprising 90% of the total data, and a hold-out dataset representing the remaining 10%. The training dataset was further split into 67% for training the base models and 33% for training the meta-learner (Figure 7). To ensure better comparison and analysis, the data underwent scaling using the Standard Scaler function in Python, which standardized the variables by removing the mean and scaling to unit variance. Notably, the chronological order of the dataset splits was preserved, with the training data containing the earliest timesteps (Figure 8) and the testing data containing the most recent timesteps.

The base learner models were trained using 67% of the training dataset, and a k-fold cross-validation approach (with k=3) was employed to estimate the optimal training parameters. The meta-learner training dataset (33% of the training dataset) was then used to generate predictions from each trained base model for the target variables, significant wave height, and average wave period (Figure 8). Initially, we trained the base learner models and then generated a meta-training dataset using predictions from the base learner models alongside the actual target values. This dataset was then employed for the training of the linear regression meta-model. During the training of the meta-learner (model), each row of the meta-training dataset contained the predictions made by base learner models for a specific sample, and at the same time, we had the actual target values for those samples. In essence, we trained the linear regression model using the predictions from base learner models as input features and the actual target values as the target variable.

Hyperparameter tuning was performed on the three base models to optimize their performance (Table 3). Hyperparameter optimization plays a crucial role in fine-tuning the behavior of machine learning models to achieve optimal results and minimize error metrics. In the final step, the hold-out test dataset (10% of the total data) was provided to the trained base models to generate their predictions for the target variables within the hold-out test dataset. These predictions were then fed into the trained meta-learner to produce the stacked model's predictions of the target values. The ensemble model, along with the three base models, was utilized for short-term (1, 3, 6, and 12 h) forecasts of significant wave height and average wave period.

Accepted for publication in *Artificial Intelligence for the Earth Systems.* DOI 10.1175/AIES-D-23-0061.1.

TABLE 3. Summary of the hyperparameters for the three base models.

Model	Model Hyperparameters
Lasso Regression	fit_intercept = 1 alpha = 0.01 max_iter = 10000 random_state = 8 Regularization= L1
Multilayer Perceptron (MLP)	Activation = identity, Alpha = 0.001 hidden_layer_sizes = (24, 24) max_iter = 20000 random_state = 8 solver = adam
Support Vector Machine (SVM)	Kernel = rbf Gamma = auto C = 0.07 max_iter = 30000

In SVM, rbf is the radial basis function, and C is the regularization parameter. Default values were used for the unspecified parameters.

We employed a standard desktop CPU for model training and forecasting. The 20-year processing required approximately 30 minutes for each model.

Accepted for publication in *Artificial Intelligence for the Earth Systems.* DOI 10.1175/AIES-D-23-0061.1.

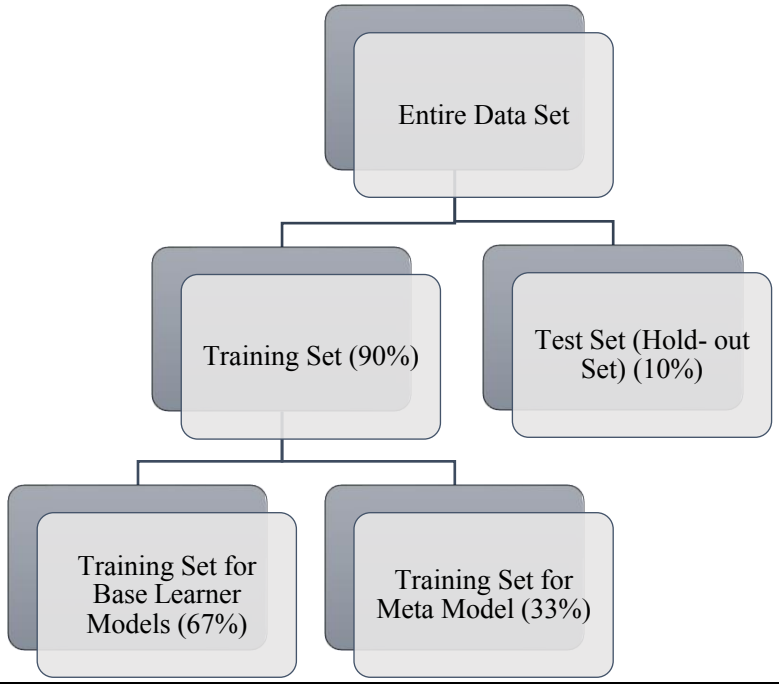

FIG. 7. Flowchart of the training set and test set.

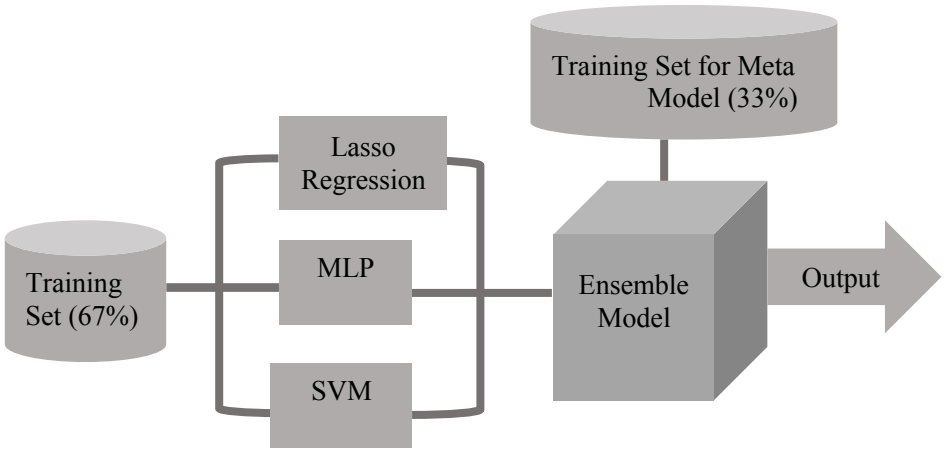

FIG. 8. Flowchart of the developed ensemble model.

d. Evaluation metrics

The models' performance and prediction accuracy were evaluated using the Coefficient of Determination (R^2), Root Mean Squared Error (RMSE), Mean Absolute Error (MAE), and the slope of the best-fit line. R^2 represents the models' performance and measures how well the model fits the data. Its value ranges between 0 and 1. Higher values indicate better model performance in capturing the variation in the data. Additionally, the slope of the best-fit line provides insights into

Accepted for publication in *Artificial Intelligence for the Earth Systems.* DOI 10.1175/AIES-D-23-0061.1.

the direction and strength of the relationship between the variables. A slope closer to 1 suggests a stronger linear relationship between the variables being analyzed.

$$R^2 = 1 - \frac{\sum(y_i - \hat{y})^2}{\sum(y_i - \bar{y})^2}$$

RMSE measures the error rate, which is calculated as the square root of the mean squared error. It estimates the average magnitude of the errors between the predicted and actual values.

$$RMSE = \sqrt{\frac{1}{N}\sum_{i=1}^{N}(y_i - \hat{y})^2}$$

MAE represents the average of all absolute errors, indicating the overall accuracy of the predictions. It is computed by averaging the absolute difference between the predicted and actual values.

$$\text{MAE} = \frac{1}{N}\sum_{i=1}^{N}|y_i - \hat{y}|$$

where $\hat{y}$ is a predicted value of y, $\bar{y}$ is a mean value of y, and N is the number of points.

4. Results and Discussion

a. Evaluating model performance

The primary goal of this study is to evaluate the performance of various ML techniques in wave forecasting within the study region, while also validating the performance of an ensemble model developed through the stacking technique. To achieve this, significant wave height and average wave period forecasts were made for forecast times of 1, 3, 6, and 12 hours at two NDBC stations on the U.S. East Coast. Three base learner models and the ensemble model were employed in the forecasting process. The forecasted parameters from each model were then compared with the observations at each buoy, and model performance statistics were analyzed.

Scatterplots display the comparisons of forecasted significant wave height (Figure 9) and average wave period (Figure 10) to observations for the forecast times using the base learner models and the ensemble model, with observations from station 41025. The results show that the ensemble model consistently outperforms the individual base learner models across all forecast times for both targets. This superiority of the ensemble model is seen numerically in the evaluation metrics in each plot box.

Accepted for publication in *Artificial Intelligence for the Earth Systems.* DOI 10.1175/AIES-D-23-0061.1.

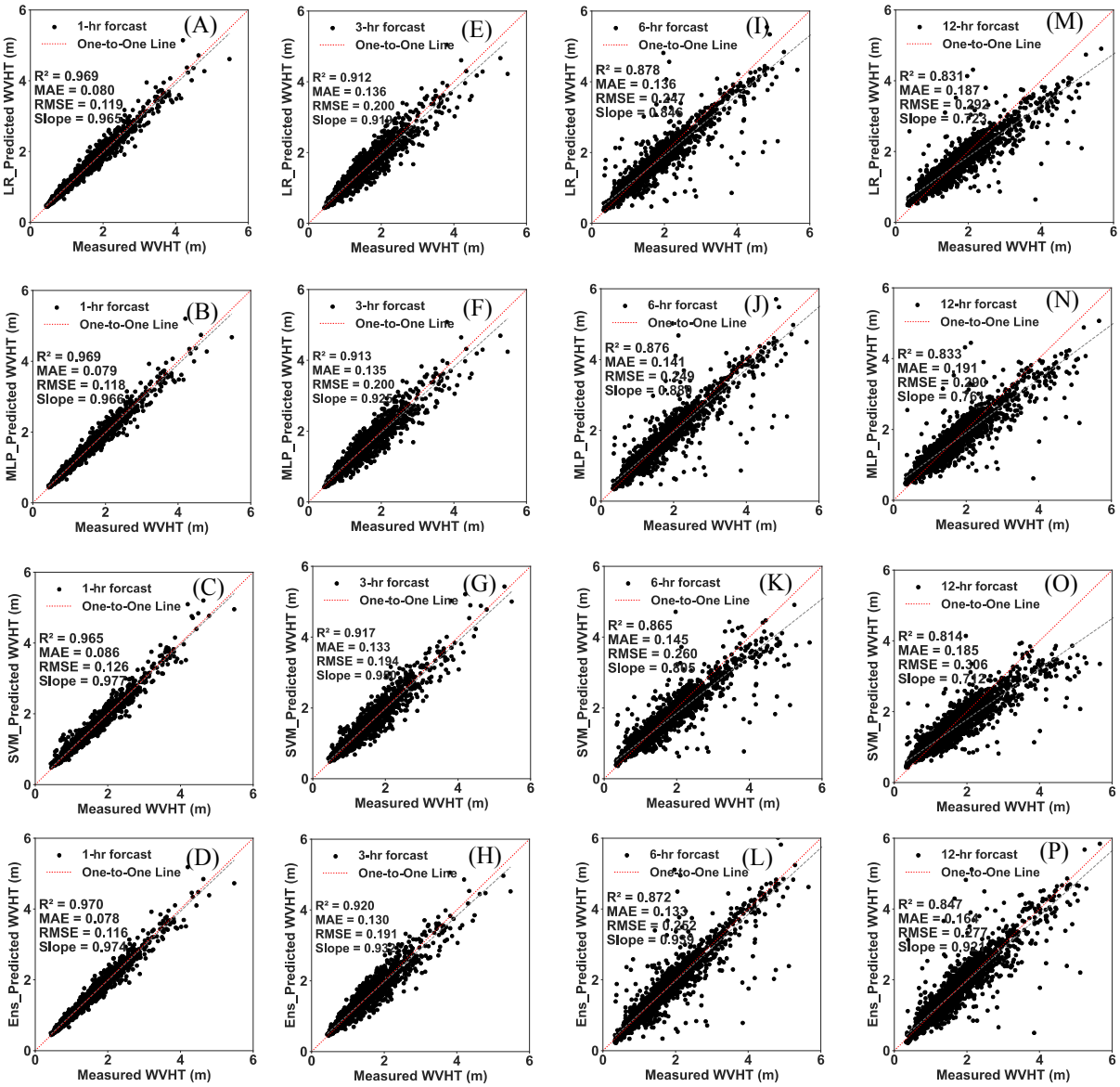

FIG. 9. Comparison of predicted 1 h (A-D), 3 h (E-H), 6 h (I-L), and 12 h (M-P) to observed significant wave height using base learner and ensemble models at NDBC station 41025. Red dashed lines represent the one-to-one relationship, and the dotted gray lines depict the best fit.

Accepted for publication in *Artificial Intelligence for the Earth Systems.* DOI 10.1175/AIES-D-23-0061.1.

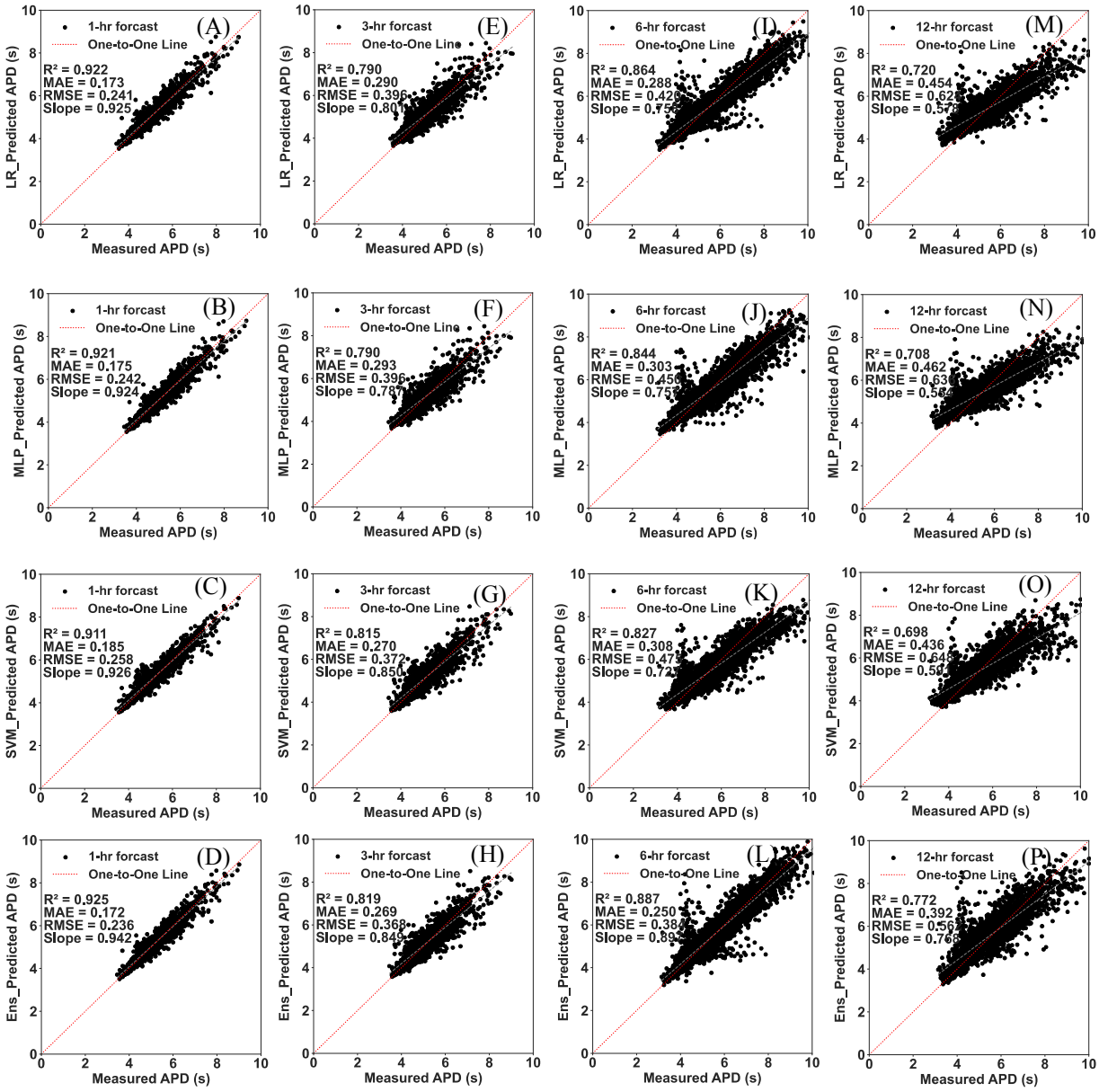

FIG. 10. Comparison of forecasted to observed average wave period for 1 h (A-D), 3 h (E-H), 6 h (I-L), and 12 h (M-P) using base learner and ensemble models at NDBC station 41025. Red dashed lines represent the one-to-one relationship, and the dotted gray lines depict the best fit.

Timeseries plots of comparisons between the ensemble model's significant wave height forecasts and the corresponding observed data at station 41025 illustrate discrepancies between the forecast and the observed data increase as the forecast lead time increases (Figure 11). This indicates that the accuracy of the ensemble model decreases as the forecast horizon extends further into the future.

Accepted for publication in *Artificial Intelligence for the Earth Systems.* DOI 10.1175/AIES-D-23-0061.1.

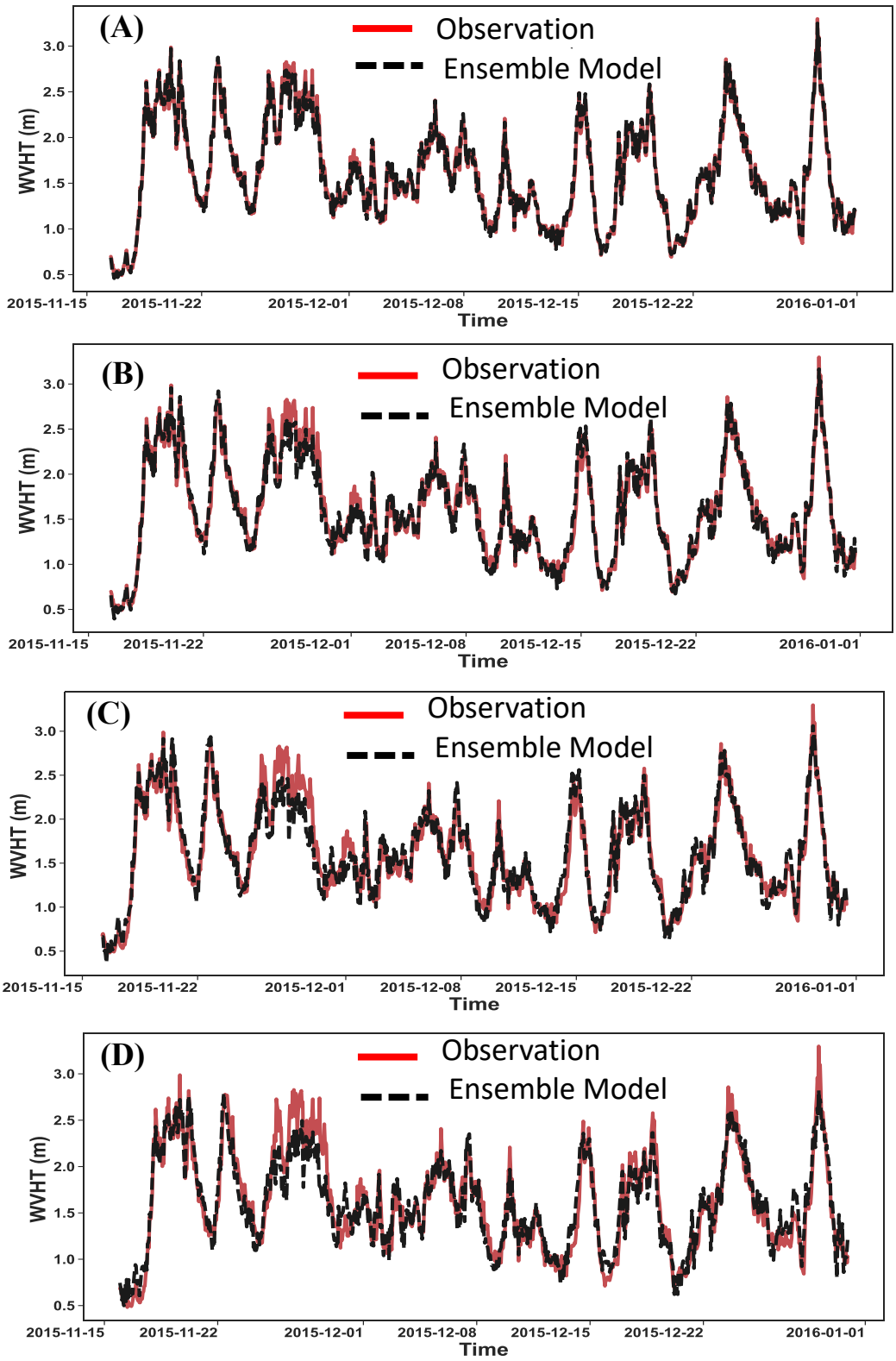

FIG. 11. An example showing the comparison of forecasted to observed significant wave height (WVHT) for (A) 1 h, (B) 3 h, (C) 6 h, and (D) 12 h at NDBC station 41025.

Accepted for publication in *Artificial Intelligence for the Earth Systems*. DOI 10.1175/AIES-D-23-0061.1.

Figures 12 and 13 display the comparisons between the significant wave height and average wave period forecasts for 1, 3, 6, and 12 hours using both the base learner models and the ensemble model, with the corresponding observed data at station 41013. For the 1-hour forecast of significant wave height at stations 41013 and 41025, the individual base learner and ensemble models exhibited satisfactory performance, with R^2 values exceeding 90% (Figures 9A-D and 12A-D). MLP performed comparably to the ensemble model ($R^2 = 0.976$) but achieved slightly higher RMSE and MAE values at station 41013 for the 1-hour forecast. Among the base learner models, Lasso Regression outperformed MLP and SVM for the significant wave height forecast (except the 1-hour forecast). Notably, SVM exhibited the least favorable performance in the majority of cases, except for the 1-hour forecast, where it achieved a higher R^2 and lower RMSE and MAE values compared to Lasso Regression (Figure 12).

The accuracy of both the base learner mode and the ensemble model exhibits a decline as the forecast horizon extends further into the future. Furthermore, the ensemble model surpassed all base learner models, exhibiting higher R^2 and smaller RMSE and MAE values in forecasting the average wave period (Figure 13A-D).

Furthermore, the ensemble model yielded a 6.5% improvement in predicted R^2 values for the 12-hour forecast of significant wave height compared to those of Lasso Regression (Figure 12M-P). Overall, the ensemble model demonstrated superior performance compared to the individual base learner models in forecasting both significant wave height and average wave period, as evidenced by the evaluation metrics R^2, RMSE, MAE, and slope of the best-fit line.

Accepted for publication in *Artificial Intelligence for the Earth Systems.* DOI 10.1175/AIES-D-23-0061.1.

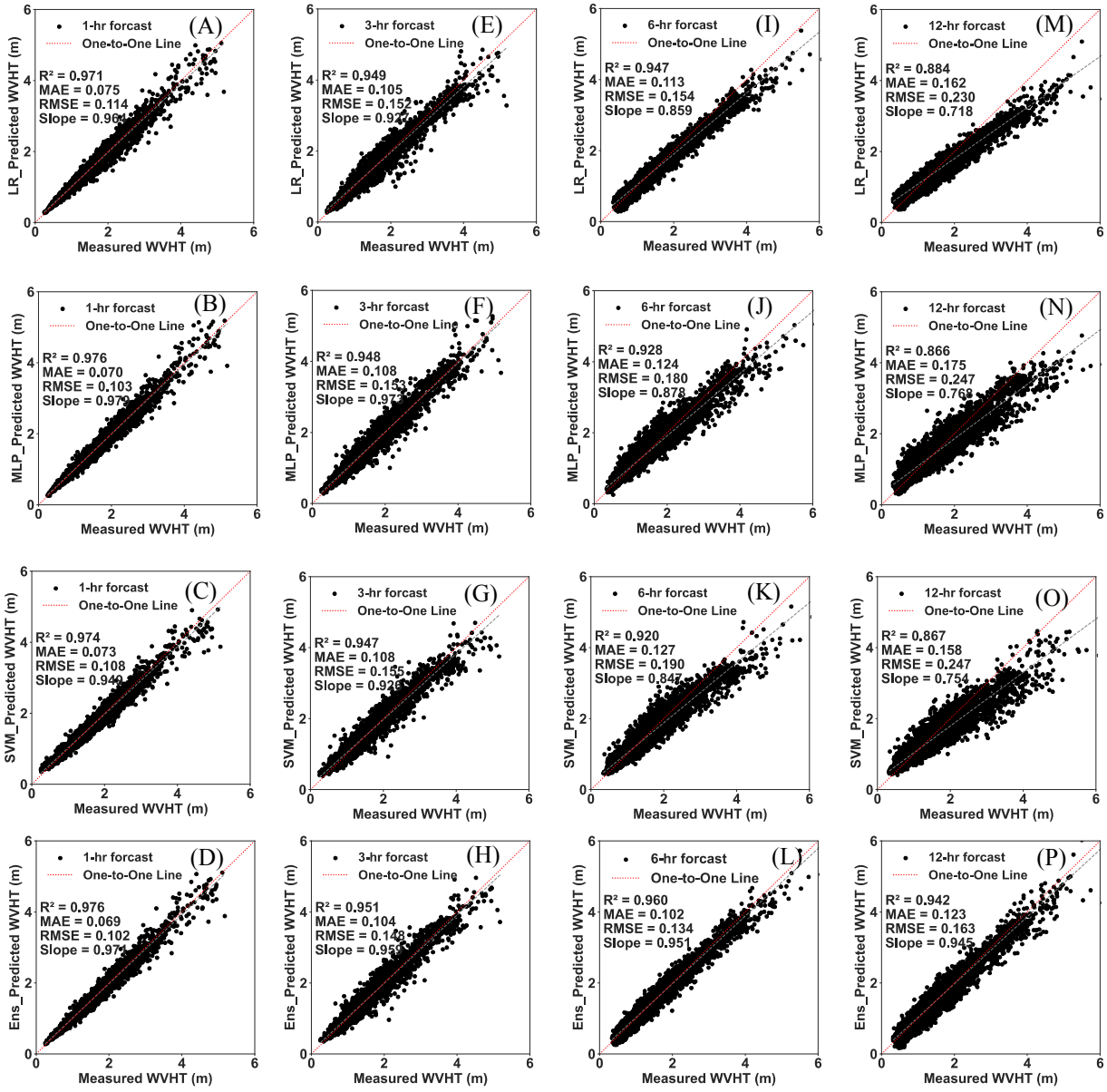

12. Comparison of forecasted to observed significant wave height (WVHT) for 1 h (A-D), 3 h (E-H), 6 h (I-L), and 12 h (M-P) using base learner and ensemble models at NDBC station 41013. Red dashed lines represent the one-to-one relationship, and the dotted gray lines depict the best fit.

Accepted for publication in *Artificial Intelligence for the Earth Systems.* DOI 10.1175/AIES-D-23-0061.1.

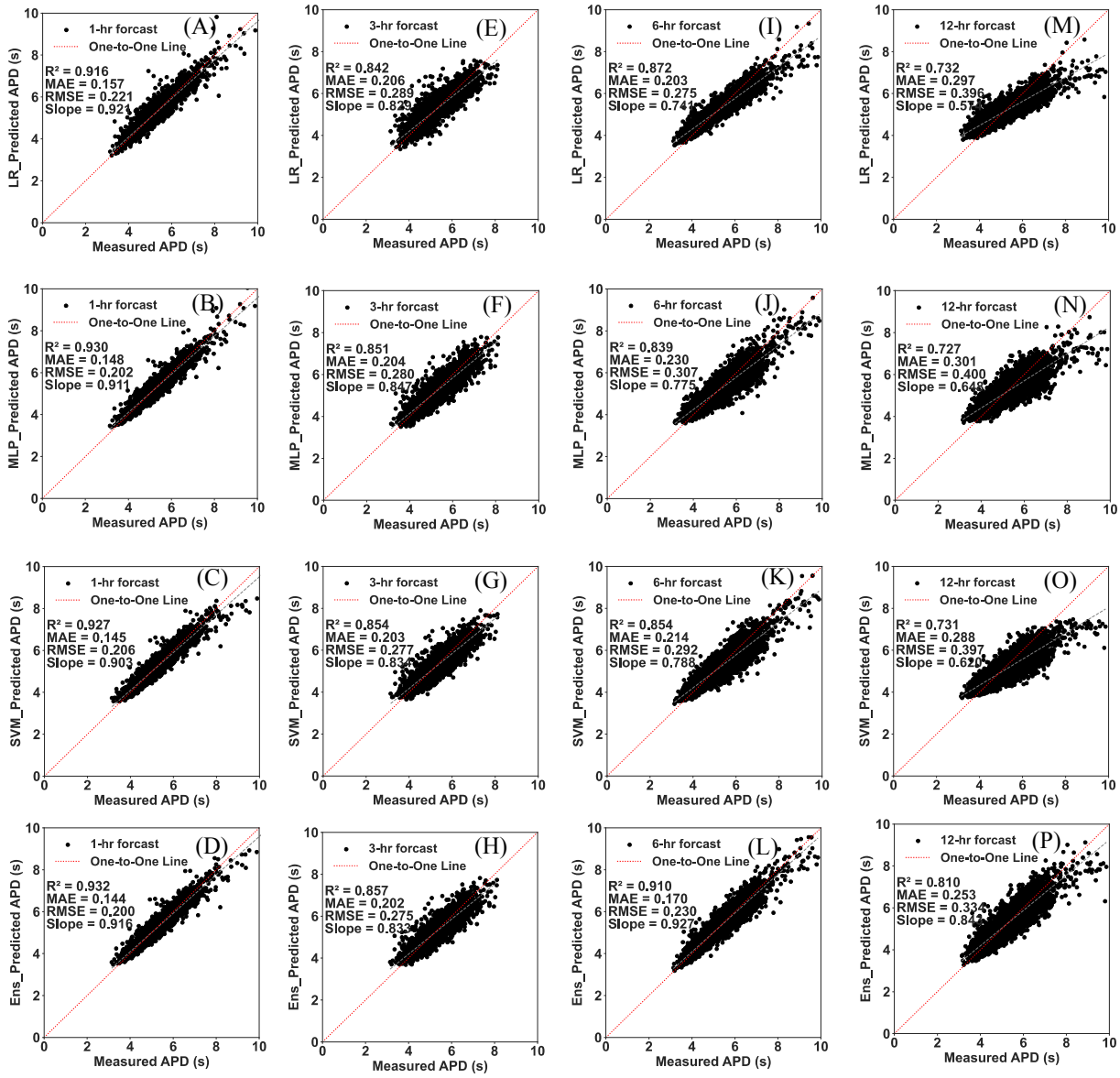

FIG. 13. Comparison of forecasted to observed average wave period (APD) for 1 h (A-D), 3 h (E-H), 6 h (I-L), and 12 h (M-P) using base learner and ensemble models at NDBC station 41013. Red dashed lines represent the one-to-one relationship, and the dotted gray lines depict the best fit.

As observed here, the accuracy of the significant wave height forecast for station 41013 is higher than that of 41025 for all the forecasts. In fact, for an extensive region like the U.S. East Coast, we expect to get different accuracies at different buoy locations when using either a numerical model or a machine learning framework (Allahdadi et al., 2019b). This non-uniform accuracy may stem from various factors, including non-uniformity of the wind field, complex model F, and different strengths of correlation between wave parameters and wind speed at different locations.

Accepted for publication in *Artificial Intelligence for the Earth Systems*. DOI 10.1175/AIES-D-23-0061.1.

In cases involving complex coastal geometry, such as the slanting fetch effect (see Allahdadi et al., 2019a), it will modify the directional spectrum and dissipate some portions of wave energy.

Evaluation metrics R^2 and RMSE for significant wave height and average wave period forecasts at station 41025 also show that the ensemble outperforms the base learner models (Figure 14), except in two cases for 1 and 6-hour forecast, where MLP yielded smaller RMSE compared to the base learner models and the ensemble model (Figure 14B). Among the base learner models, Lasso Regression exhibited slightly higher R^2 for significant wave height at all forecast times (Figure 14A). Similarly, Lasso Regression showed the best overall performance for average wave period forecasts, with SVM yielding slightly higher R^2 and smaller RMSE for the 3 and 12-hour forecast (Figure 14C-D). As seen in other metrics, the ensemble model consistently improved forecast accuracy for both target parameters and across most forecast times, with higher R^2 values and lower RMSE values.

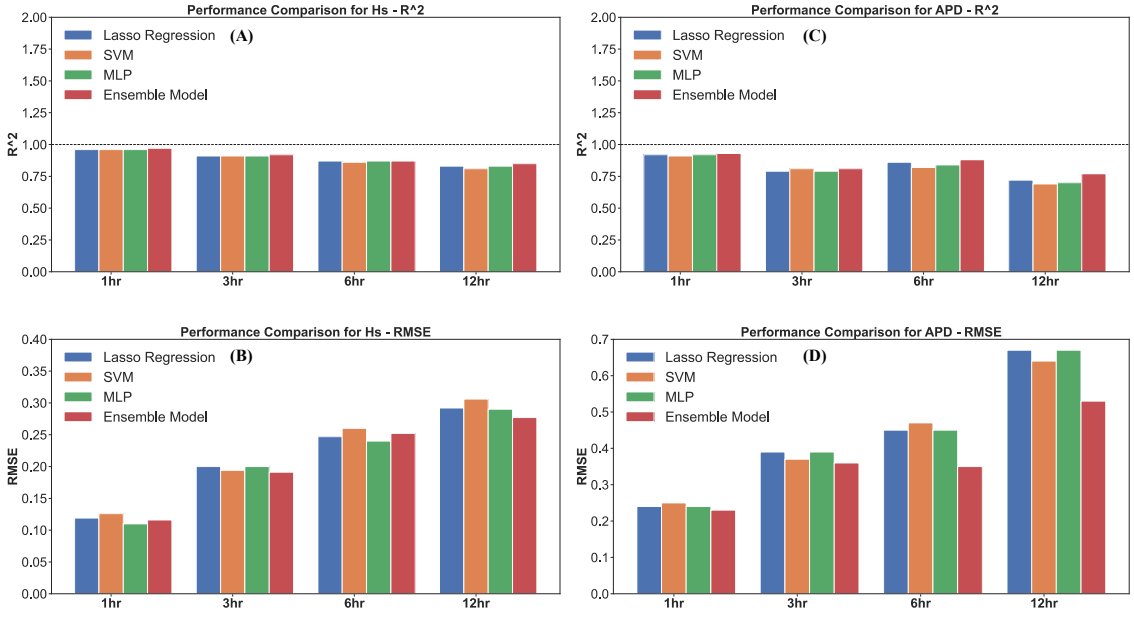

FIG. 14. R^2 and RMSE between forecasted and observed significant wave height (A and B) and average wave period (C and D) at 1, 3, 6, and 12 h forecast times. The forecasts were generated using base learner models Lasso Regression (blue), SVM (orange), MLP (green), and the ensemble model (red) at NDBC station 41025.

b. Effect of including swells in analysis

The impact of including swells wave height in model training was investigated for forecast times of 1 to 12 hours at both stations. The results indicate that the effect of swells on forecast accuracy was negligible for forecast times of 6 hours or less, but became significant for the 12-hour

Accepted for publication in *Artificial Intelligence for the Earth Systems*. DOI 10.1175/AIES-D-23-0061.1.

forecast. For example, on December 24, 2015, at 2:00 AM at station 41013, including in the inputs swells that occurred 6 hours prior resulted in a 4.4% reduction in the difference between the forecasted and observed values for the 12-hour significant wave height forecast. At that time, the measured significant wave height was approximately 2.98 m, which is relatively high. Similarly, on November 27, 2015, at 4:00 PM at station 41025, including swells from the past 12 hours resulted in an improvement from a 12.2% difference between forecasted without swells and observed to a 9.3% difference between forecasted with swells and observed. The measured significant wave height at that time was approximately 2.82 m. These examples highlight the positive impact of incorporating swells into the analysis, improving the accuracy of predicting significant wave height for the 12-hour forecast.

Incorporating swells and seas as input features in the ensemble model improved the prediction of significant wave height for the 12-hour forecast (Figure 15). R^2 increased from 0.80 without to 0.84 with swells and seas, indicating a better fit between the predicted and measured values. Additionally, MAE and RMSE decreased by up to 0.03 m, showing that the inclusion of swells and seas reduced forecast errors. The forecasted significant wave height, with and without considering the swells height, was more accurate during peaks, suggesting that the inclusion of swells enhanced the model's ability to capture and predict extreme wave events accurately.

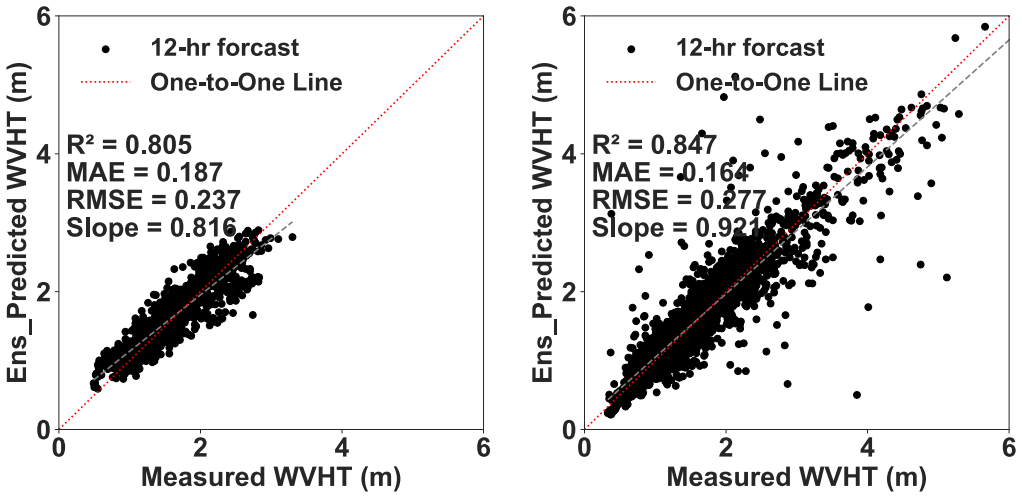

FIG. 15. Comparison of significant wave height (WVHT) without (A) and with (B) swells and seas as input features at NDBC station 41025. Red dashed lines represent the one-to-one relationship, and the dotted gray lines depict the best fit.

Accepted for publication in *Artificial Intelligence for the Earth Systems*. DOI 10.1175/AIES-D-23-0061.1.

5. Summary and conclusion

We developed and evaluated an ensemble model to forecast significant wave height and average wave period for various forecast times (1, 3, 6, and 12 h) at two NOAA National Data Buoy Center (NDBC) stations along the U.S. Atlantic coast. We collected a comprehensive dataset spanning almost 20 years that included meteorological variables and wave parameters to train and test our model.

Through careful feature selection, we identified relevant variables that played key roles in predicting wave parameters. Additionally, we conducted a swell component analysis to account for the contribution of swells generated by remote winds. By separating the swell component from the overall wave energy spectrum, we included it as an independent predictor in our analysis. We employed three base learner models: Lasso Regression, Support Vector Machine (SVM), and Multi-Layer Perceptron (MLP), which are known for their effectiveness in wave parameter forecasting. These models captured the complex relationships between the selected features and the target variables. To further enhance prediction accuracy, we developed an ensemble model using the stacking method. The ensemble model combined the predictions from the base learner models through a meta-learner, which learned how to combine these predictions to generate the final prediction effectively.

The ensemble model outperformed the individual base learner models in predicting significant wave height and average wave period. The ensemble model demonstrated higher accuracy and reliability, as evidenced by evaluation metrics Coefficient of Determination (R^2), Root Mean Squared Error (RMSE), and Mean Absolute Error (MAE). The greatest model accuracy was achieved by leveraging the strengths of multiple models and incorporating the swell component.

Overall, our findings suggest that the ensemble model developed in this study can be a valuable tool for forecasting wave parameters along the U.S. Atlantic coast and potentially other ocean regions. This ensemble model offers improved accuracy and robustness compared to individual models, providing a promising alternative to computing-intensive traditional coastal models. Future research could explore the application of the ensemble model for long-term wave parameter forecasts and investigate spatial-temporal predictions of wave parameters.

In conclusion, our study contributes to wave forecasting by developing a machine learning ensemble model that effectively predicts significant wave height and average wave period while using far less computational resources than traditional ocean models. The findings highlight the

Accepted for publication in *Artificial Intelligence for the Earth Systems.* DOI 10.1175/AIES-D-23-0061.1.

potential of the ensemble model for enhancing wave parameter forecasts, offering valuable insights for coastal planning and management, wave energy development, port infrastructure, fishery activities, maritime security, and offshore wind energy and oil and gas asset design and operations.

Acknowledgments

Research support provided through NSF grant ICER-2019758, OCE-1851421, and NOAA grant NA16NOS0120028 is much appreciated. We thank Jennifer Warrillow for her editorial assistance.

Data and Code Availability Statement

Meteorological, wave parameter, and wave spectral data were collected from January 1, 2012, to December 31, 2015, from two stations operated by the NOAA National Data Buoy Center and are available at: https://www.ndbc.noaa.gov/. Model codes and output are available upon request. A part of the code used in this study was adapted from two external sources (Tan, 2021): https://towardsdatascience.com/stacking-machine-learning-models-for-multivariate-time-series-28a082f881 and https://github.com/at-tan/Forecasting_Air_Pollution

References:

Ahn, S., Neary, V.S., Allahdadi, M.N., He, R., 2021. Nearshore wave energy resource characterization along the East Coast of the United States. Renewable Energy 172, 1212–1224. https://doi.org/10.1016/j.renene.2021.03.037

Ahn, S., Tran, T.D., Kim, J., 2022. Systematization of short-term forecasts of regional wave heights using a machine learning technique and long-term wave hindcast. Ocean Engineering 264, 112593. https://doi.org/10.1016/j.oceaneng.2022.112593

Allahdadi, M.N., Chaichitehrani, N., Allahyar, M., McGee, L., 2017. Wave Spectral Patterns during a Historical Cyclone: A Numerical Model for Cyclone Gonu in the Northern Oman Sea. Open Journal of Fluid Dynamics 7, 131–151. https://doi.org/10.4236/ojfd.2017.72009

Allahdadi, M.N., He, R., Neary, V.S., 2019. Predicting ocean waves along the US east coast during energetic winter storms: sensitivity to whitecapping parameterizations. Ocean Science 15, 691–715. https://doi.org/10.5194/os-15-691-2019

Allahdadi, M.N., Gunawan, B., Lai, J., He, R., Neary, V.S., 2019. Development and validation of a regional-scale high-resolution unstructured model for wave energy resource characterization along the US East Coast. Renewable Energy 136, 500–511. https://doi.org/10.1016/j.renene.2019.01.020

Alsmadi, M. khalil, Omar, K.B., Noah, S.A., Almarashdah, I., 2009. Performance Comparison of Multi-layer Perceptron (Back Propagation, Delta Rule and Perceptron) algorithms in Neural Networks, in: 2009 IEEE International Advance Computing Conference. Presented at the 2009 IEEE International Advance Computing Conference, pp. 296–299.

Ardhuin, F., Herbers, T.H.C., Watts, K.P., van Vledder, G.P., Jensen, R., Graber, H.C., 2007. Swell and Slanting-Fetch Effects on Wind Wave Growth. J. Phys. Oceanogr. 37, 908–931. https://doi.org/10.1175/JPO3039.1

Ardhuin, F., Chapron, B., Collard, F., 2009. Observation of swell dissipation across oceans. Geophysical Research Letters 36. https://doi.org/10.1029/2008GL037030

Accepted for publication in *Artificial Intelligence for the Earth Systems*. DOI 10.1175/AIES-D-23-0061.1.

Berbić, J., Ocvirk, E., Carevic, D., Loncar, G., 2017. Application of neural networks and support vector machine for significant wave height prediction. Oceanologia 59. https://doi.org/10.1016/j.oceano.2017.03.007

Berkhahn, S., Fuchs, L., Neuweiler, I., 2019. An ensemble neural network model for real-time prediction of urban floods. Journal of Hydrology 575, 743–754. https://doi.org/10.1016/j.jhydrol.2019.05.066

Booij, N., Ris, R.C., Holthuijsen, L.H., 1999. A third-generation wave model for coastal regions: 1. Model description and validation. Journal of Geophysical Research: Oceans 104, 7649–7666. https://doi.org/10.1029/98JC02622

Chaichitehrani, N., Allahdadi, M.N., 2018. Overview of Wind Climatology for the Gulf of Oman and the Northern Arabian Sea. American Journal of Fluid Dynamics 8, 1–9.

Chaichitehrani, N., Allahdadi, M.N., Li, C., 2022. Simulation of Low Energy Waves during Fair-Weather Summer Conditions in the Northern Gulf of Mexico: Effect of Whitecapping Dissipation and the Forcing Accuracy. Atmosphere 13, 2047. https://doi.org/10.3390/atmos13122047

Dawson, H.L., Dubrule, O., John, C.M., 2023. Impact of dataset size and convolutional neural network architecture on transfer learning for carbonate rock classification. Computers & Geosciences 171, 105284. https://doi.org/10.1016/j.cageo.2022.105284

de Farias, E.G.G., Lorenzzetti, J.A., Chapron, B., 2012. Swell and Wind-Sea Distributions over the Mid-Latitude and Tropical North Atlantic for the Period 2002–2008. International Journal of Oceanography 2012, e306723. https://doi.org/10.1155/2012/306723

Dietterich, T.G., 2000. Ensemble Methods in Machine Learning, in: Multiple Classifier Systems, Lecture Notes in Computer Science. Springer, Berlin, Heidelberg, pp. 1–15. https://doi.org/10.1007/3-540-45014-9_1

Elbisy, M.S., 2015. Sea Wave Parameters Prediction by Support Vector Machine Using a Genetic Algorithm. coast 31, 892–899. https://doi.org/10.2112/JCOASTRES-D-13-00087.1

Engineers, U.A.C.O., 2002. Coastal engineering manual. *Engineer Manual*, *1110*, pp.2-1100.

Fan, S., Xiao, N., Dong, S., 2020. A novel model to predict significant wave height based on long short-term memory network. Ocean Engineering 205, 107298. https://doi.org/10.1016/j.oceaneng.2020.107298

Ghadami, A., Epureanu, B.I., 2016. Bifurcation Forecasting for Large Dimensional Oscillatory Systems: Forecasting Flutter Using Gust Responses. Journal of Computational and Nonlinear Dynamics 11. https://doi.org/10.1115/1.4033920

Gracia, S., Olivito, J., Resano, J., Martin-del-Brio, B., de Alfonso, M., Álvarez, E., 2021. Improving accuracy on wave height estimation through machine learning techniques. Ocean Engineering 236, 108699. https://doi.org/10.1016/j.oceaneng.2021.108699

Gulev, S.K., Grigorieva, V., 2006. Variability of the Winter Wind Waves and Swell in the North Atlantic and North Pacific as Revealed by the Voluntary Observing Ship Data. Journal of Climate 19, 5667–5685. https://doi.org/10.1175/JCLI3936.1

Gütter, J., Kruspe, A., Zhu, X.X., Niebling, J., 2022. Impact of Training Set Size on the Ability of Deep Neural Networks to Deal with Omission Noise. Front. Remote Sens. 3. https://doi.org/10.3389/frsen.2022.932431

Hu, H., van der Westhuysen, A.J., Chu, P., Fujisaki-Manome, A., 2021. Predicting Lake Erie wave heights and periods using XGBoost and LSTM. Ocean Modelling 164, 101832. https://doi.org/10.1016/j.ocemod.2021.101832

Accepted for publication in *Artificial Intelligence for the Earth Systems.* DOI 10.1175/AIES-D-23-0061.1.

Isaie Moghaddam, E., Allahdadi, M.N., Ashrafi, A., Chaichitehrani, N., 2021. Coastal system evolution along the southeastern Caspian Sea coast using satellite image analysis: response to the sea level fall during 1994–2015. Arab J Geosci 14, 771. https://doi.org/10.1007/s12517-021-07106-2

Jain, P., Deo, M.C., Latha, G., Rajendran, V., 2011. Real time wave forecasting using wind time history and numerical model. Ocean Modelling 36, 26–39. https://doi.org/10.1016/j.ocemod.2010.07.006

James, S.C., Zhang, Y., O'Donncha, F., 2017. A Machine Learning Framework to Forecast Wave Conditions. https://doi.org/10.48550/arXiv.1709.08725

Kim, T., Adali, T., 2002. Fully Complex Multi-Layer Perceptron Network for Nonlinear Signal Processing. The Journal of VLSI Signal Processing-Systems for Signal, Image, and Video Technology 32, 29–43. https://doi.org/10.1023/A:1016359216961

Kruse, R., Mostaghim, S., Borgelt, C., Braune, C., Steinbrecher, M., 2022. Multi-layer Perceptrons, in: Kruse, R., Mostaghim, S., Borgelt, C., Braune, C., Steinbrecher, M. (Eds.), Computational Intelligence: A Methodological Introduction, Texts in Computer Science. Springer International Publishing, Cham, pp. 53–124. https://doi.org/10.1007/978-3-030-42227-1_5

Kumar, N.K., Savitha, R., Al Mamun, A., 2018. Ocean wave height prediction using ensemble of Extreme Learning Machine. Neurocomputing, Hierarchical Extreme Learning Machines 277, 12–20. https://doi.org/10.1016/j.neucom.2017.03.092

Li, N., Cheung, K.F., Cross, P., 2020. Numerical wave modeling for operational and survival analyses of wave energy converters at the US Navy Wave Energy Test Site in Hawaii. Renewable Energy 161, 240–256. https://doi.org/10.1016/j.renene.2020.06.089

Londhe, S.N., Panchang, V., 2006. One-Day Wave Forecasts Based on Artificial Neural Networks. Journal of Atmospheric and Oceanic Technology 23, 1593–1603. https://doi.org/10.1175/JTECH1932.1

Mahjoobi, J., Adeli Mosabbeb, E., 2009. Prediction of significant wave height using regressive support vector machines. Ocean Engineering 36, 339–347. https://doi.org/10.1016/j.oceaneng.2009.01.001

Martins, S., Bernardo, N., Ogashawara, I., Alcantara, E., 2016. Support Vector Machine algorithm optimal parameterization for change detection mapping in Funil Hydroelectric Reservoir (Rio de Janeiro State, Brazil). Model. Earth Syst. Environ. 2, 138. https://doi.org/10.1007/s40808-016-0190-y

Massel, Stanislaw. R. 1996. Ocean Surface Waves: Their Physics and Prediction, world scientific. Pages: 508

Moghaddam, E.I., Hakimzadeh, H., Allahdadi, M.N., Hamedi, A., Nasrollahi, A., 2018. Wave-induced Currents in the Northern Gulf of Oman: A Numerical Study for Ramin Port along the Iranian Coast. American Journal of Fluid Dynamics 8, 30–39.

Mooneyham, J., Crosby, S.C., Kumar, N., Hutchinson, B., 2020. SWRL Net: A Spectral, Residual Deep Learning Model for Improving Short-Term Wave Forecasts. Weather and Forecasting 35, 2445–2460. https://doi.org/10.1175/WAF-D-19-0254.1

Pirhooshyaran, M., Snyder, L.V., 2020. Forecasting, hindcasting and feature selection of ocean waves via recurrent and sequence-to-sequence networks. Ocean Engineering 207, 107424. https://doi.org/10.1016/j.oceaneng.2020.107424

Accepted for publication in *Artificial Intelligence for the Earth Systems.* DOI 10.1175/AIES-D-23-0061.1.

Sadeghifar, T., Nouri Motlagh, M., Torabi Azad, M., Mohammad Mahdizadeh, M., 2017. Coastal Wave Height Prediction using Recurrent Neural Networks (RNNs) in the South Caspian Sea. Marine Geodesy 40, 454–465. https://doi.org/10.1080/01490419.2017.1359220

Salcedo-Sanz, S., Rojo-Álvarez, J.L., Martínez-Ramón, M., Camps-Valls, G., 2014. Support vector machines in engineering: an overview. WIREs Data Mining and Knowledge Discovery 4, 234–267. https://doi.org/10.1002/widm.1125

Sapiega, P., Zalewska, T., Struzik, P., 2023. Application of SWAN model for wave forecasting in the southern Baltic Sea supplemented with measurement and satellite data. Environmental Modelling & Software 163, 105624. https://doi.org/10.1016/j.envsoft.2023.105624

Tan, A.T., 2021. Stacking Machine Learning Models for Multivariate Time Series. Towards Data Science. https://towardsdatascience.com/stacking-machine-learning-models-for-multivariate-time-series-28a082f881

Tolman, H.L., Chalikov, D., 1996. Source Terms in a Third-Generation Wind Wave Model. Journal of Physical Oceanography 26, 2497–2518. https://doi.org/10.1175/1520-0485(1996)026<2497:STIATG>2.0.CO;2

Wei, Z., 2021. Forecasting wind waves in the US Atlantic Coast using an artificial neural network model: Towards an AI-based storm forecast system. Ocean Engineering 237, 109646. https://doi.org/10.1016/j.oceaneng.2021.109646

Zounemat-Kermani, M., Matta, E., Cominola, A., Xia, X., Zhang, Q., Liang, Q., Hinkelmann, R., 2020. Neurocomputing in surface water hydrology and hydraulics: A review of two decades retrospective, current status and future prospects. Journal of Hydrology 588, 125085. https://doi.org/10.1016/j.jhydrol.2020.125085

Zhan, Y., Zhang, H., Li, J., Li, G., 2022. Prediction Method for Ocean Wave Height Based on Stacking Ensemble Learning Model. Journal of Marine Science and Engineering 10, 1150. https://doi.org/10.3390/jmse10081150

Accepted for publication in *Artificial Intelligence for the Earth Systems.* DOI 10.1175/AIES-D-23-0061.1.